CRREL Permafrost Tunnel
Fox, Alaska

A Guidebook

prepared by the:

Institute of Northern Engineering
University of Alaska Fairbanks
P.O. Box 755910
Fairbanks, Alaska 99775-5910

LATE-PLEISTOCENE SYNGENETIC PERMAFROST IN THE CRREL PERMAFROST TUNNEL, FOX, ALASKA

M. Z. Kanevskiy, H. M. French, and Y. L. Shur (eds.)

CONTRIBUTING AUTHORS:
Bjella, K.L.[1], Bray, M.T.[2], Collins, C.M.[1], Douglas, T.A.[1], Fortier, D.[2], French, H.M.[3], Kanevskiy, M.Z.[2], Shur, Y.L.[2]

[1]CRREL, [2]University of Alaska Fairbanks, [3]University of Ottawa, Canada

ABSTRACT

Late-Pleistocene syngenetic permafrost exposed in the walls and ceiling of the CRREL permafrost tunnel consists of ice- and organic-rich silty sediments penetrated by ice wedges. Evidence of long-continued syngenetic freezing under cold-climate conditions includes the dominance of lenticular and micro-lenticular cryostructures throughout the walls, ice veins and wedges at many levels, the presence of undecomposed rootlets, and organic-rich layers that reflect the former positions of the ground surface. Fluvio-thermal modifications are indicated by bodies of thermokarst-cave ('pool') ice, by soil and ice pseudomorphs, and by reticulate-chaotic cryostructures associated with freezing of saturated sediments trapped in underground channels.

INTRODUCTION

The CRREL permafrost tunnel is located at Fox, approximately 16 km north of Fairbanks, Alaska. Constructed 40 years ago, it is one of the few underground exposures of syngenetic Pleistocene-age permafrost. Naturally-occurring exposures of ice-rich permafrost quickly degrade and provide only opportunistic study. The permafrost tunnel allows hundreds of visitors the unhurried opportunity to become acquainted with ice-rich permafrost, and for professionals to study the peculiarities of syngenetic permafrost and its history.

This guide summarizes recent cryostratigraphic observations made from within the tunnel and re-evaluates earlier interpretations. Some observations have been described in previous publications (e.g. Shur et al. 2004, Bray et al. 2006) while others are presented in the NICOP proceedings volume (e.g. Bray 2008, Fortier et al. 2008, Kanevskiy et al. 2008).

THE CRREL TUNNEL

The CRREL permafrost tunnel was constructed in the early 1960's by the U.S. Army Cold Regions Research and Engineering Laboratory (CRREL) in order to test mining, tunneling, and construction techniques in permafrost. It continues to be maintained by CRREL for research opportunity. The plan of the tunnel is shown in figure 1. The tunnel entrance is located on the eastern margin of Goldstream Creek Valley where a steep 10 m high escarpment had been created by placer gold mining activities in the first part of the previous century. The surface of the valley that lies immediately above the long axis of the tunnel rises gently from the top of the escarpment in which the entrance is located towards the east side of Goldstream Creek Valley. The active layer of the terrain that overlies the tunnel is between 0.7 and 1.0 m thick. This is typical of the Fairbanks area.

The tunnel is composed of two portions (see fig. 1). The adit (a nearly horizontal passage from the surface into the hillside) was driven by the U.S. Army Corps of Engineers using continuous mining methods in the winters of 1963-64, 1964-65, and 1965-66 (Sellmann 1967). The winze (an inclined adit) was driven by the U.S. Bureau of Mines (USBM) from 1968 to 1969 using drill and blast, thermal relaxation, and hydraulic relaxation methods (Chester & Frank 1969). The adit extends approximately 110 m in length and is predominantly located in the frozen silt unit. The winze begins approximately 30 m into the adit and drops obliquely at an incline of 14% for 45 m, passing into the frozen gravel unit and ultimately into the weathered bedrock, where a Gravel Room was excavated (Pettibone & Waddell 1973). At the time of excavation, portions of the Gravel Room roof consisted of

2.0 m of frozen gravel lying below the overlying silt unit. After the winze levels out adjacent to the Gravel Room, it continues for another 10 m into what is known as the CRREL Room. The tunnel is chilled by natural ventilation in winter and by artificial refrigeration in summer, supporting permafrost stability.

Many papers have been published on the geology, paleoecology, and cryostratigraphy of the sediments exposed in the tunnel (Sellmann 1967, 1972, Watanabe 1969, Hamilton et al. 1988, Long and Péwé 1996, Shur et al. 2004, Pikuta et al. 2005, Bray et al. 2006, Katayama et al. 2007, Wooler et al. 2007, Fortier et al. 2008, Kanevskiy et al. 2008) as well as their engineering properties (Chester & Frank 1969, Pettibone & Waddell 1971, 1973, Thompson & Sayles 1972, Johansen et al. 1981, Johansen & Ryer 1982, Garbeil 1983, Weerdenburg & Morgenstern 1983, Arcone & Delaney 1984, Delaney & Arcone 1984, Huang et al. 1986, Delaney 1987, Bray 2008). The problems of tunnel construction have also been described (Chester & Frank 1969, Dick 1970, Swinzow 1970, Linnell & Lobacz 1978).

Sediments exposed within the tunnel consist mainly of frozen silts that range in age from Wisconsin to Recent (fig. 2). They are eolian (i.e. wind-blown) in nature and are largely derived from the outwash gravels and braided stream deposits of the Tanana lowlands and surrounding hills. Ice-rich silts of eolian origin were also partly reworked and re-transported by slope and fluvial processes (Péwé 1975, Hamilton et al. 1988).The silts overlie fluvial gravels of Nebraskan age (Fox Gravel) that are derived from the sur¬rounding hills of the Yukon–Tanana Uplands. These gravels over¬lie Pre-Cambrian schist bedrock.

The silt overburden at the thickest point is approximately 14 m over the adit and 18 m over the Gravel Room.

Figure 1. Isometric view of the tunnel.

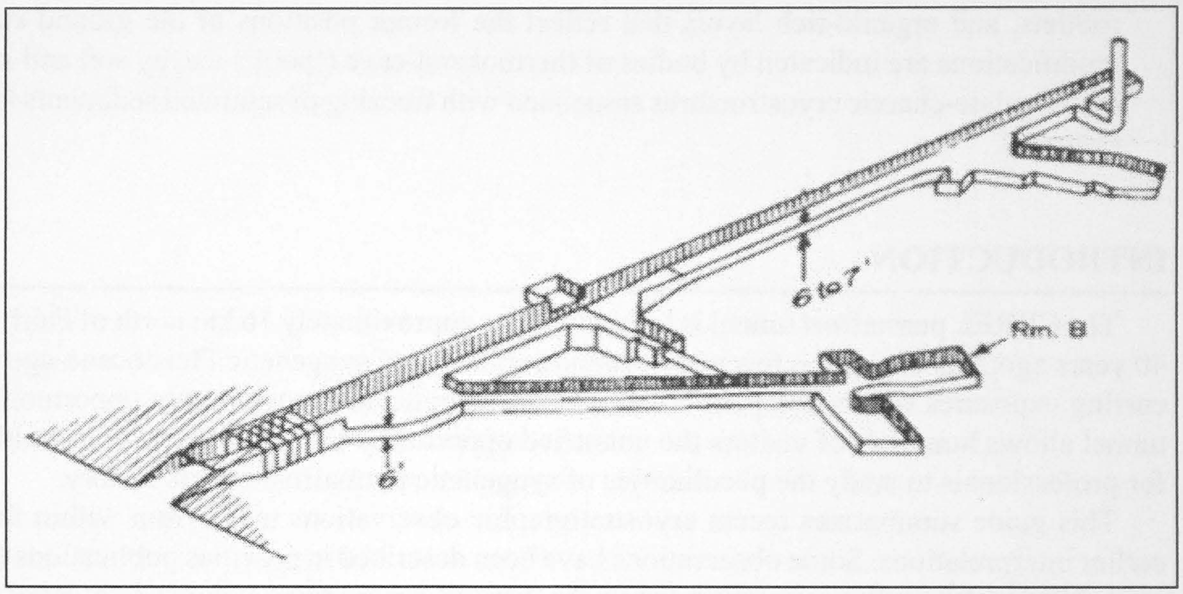

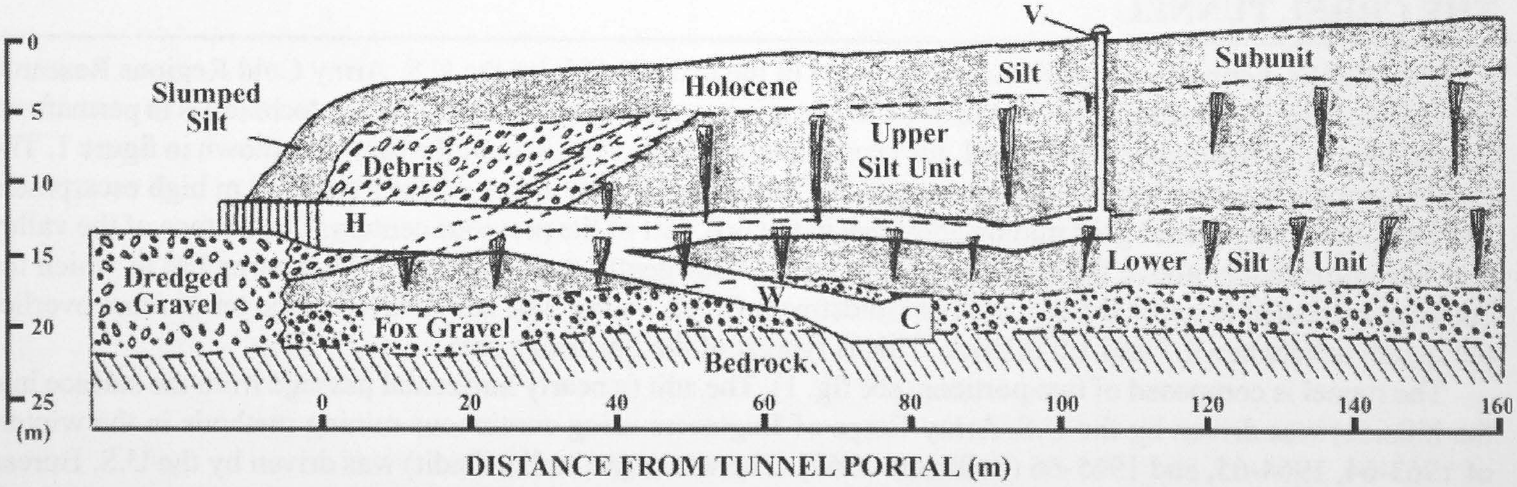

Figure 2. Cross section of the geology and permafrost features exposed in the CRREL tunnel near Fairbanks, Alaska. Two units of ice-rich Pleistocene-age silt are shown to be separated from two sets of ice wedges by an unconformity (dashed line). H—horizontal tunnel (adit); V—ventilation shaft (does not exist today); W—winze; C—chamber. (From Hamilton et al. 1988).

Near the tunnel portal, the fanlike deposits of poorly-sorted debris overlie the silts in an unconformable fashion; they formed between 12,500 and 11,000 years BP during deep erosion of the Goldstream Creek Valley slopes (Hamilton et al. 1988).

PREVIOUS OBSERVATIONS ON THE TUNNEL PERMAFROST

Sellmann (1967, 1972) was the first to provide information on the tunnel geology and permafrost. He described segregation ice, foliated wedge ice, and large clear masses of ice (buried 'aufeis'). He also identified two 'unconformities'. The upper was marked by the tops of small wedges and a change in soil color. The lower unconformity was identified by (i) a change in size and shape of wedges, (ii) a gap in radiocarbon ages obtained from organic material contained within the silty sediments in the tunnel walls of between 14,000 and 30,000 years BP, and (iii) a 20-fold increase in chemical concentration with depth. Sellmann suggested '…this unconformity was probably caused by some regional warming or local depositional or erosional event'.

Subsequently, Hamilton et al. (1988) obtained samples from the tunnel walls and reported upon 33 radiocarbon dates. The dates for silts are within the range 30,000 – 43,000 years BP. In addition, a diverse assemblage of animals' bones (bison, horse, mammoth (?), caribou (?) and arctic ground squirrel) and plant macrofossils (grasses and sedges) indicated a tundra or shrub-tundra environment. Hamilton et al. (1988) concluded that the tunnel '... provides continuous and undisturbed exposures of ice-rich silt that overlies gravel and bedrock' and that '…most of the pore and segregated ice formed during freezing of silt'. They identified pore ice, segregated ice, foliated wedge ice and buried surface ice, as previously documented by Péwé (1975) and concluded that 'most of the pore ice and segregated ice formed during freezing of silt and has been preserved since that time'. They also identified two independent systems of ice wedges and inferred a thaw unconformity between them (fig. 2). Other bodies of ice, described as '...horizontal, saucer-shaped bodies, 2–6 m wide and 0.5–2 m deep' (Hamilton et al. 1988) were interpreted as buried frozen thaw ponds formed in ice-wedge troughs. According to these authors, these ice bodies '…generally consist of 3 successive depth zones: (1) clear ice with vertical bubble trains, transitional downward into (2) ice containing reddish brown, suspended organic matter that overlies (3) a lenticular body of unusually ice-rich silt'.

CRYOSTRATIGRAPHY AND CRYOLITHOLOGY

Cryostratigraphy refers to the study of frozen layers in the Earth's crust. It is a branch of geocryology. It was developed first in Russia where the study of ground ice gained early attention (Shumskii 1959, Katasonov 1962, 1969) and subsequently led to highly detailed studies (e.g. Vtyurin 1964, Popov 1967, 1973, Gasanov 1969, Gravis 1969, Zhestkova 1982, Shur 1988, Romanovskii 1993, Dubikov 2002) that are unparalleled in North America. A summary of cryostratigraphic principles can be found in French (2007, 153-185).

Cryostratigraphy differs from traditional stratigraphy by specifically recognizing that perennially-frozen sediment and rock contain structures that are different to those found in unfrozen sediment and rock. Cryolithology is a related branch of geocryology and refers to the relationship between the lithological characteristics of rocks and their ground ice amounts and distribution. The structures, largely determined by the amount and distribution of ice within sediments are termed 'cryostructures'. Cryostructures are useful in determining the nature of the freezing process and the conditions under which frozen sediment accumulates.

A distinction must be made between epigenetic and syngenetic permafrost (fig. 3). Epigenetic permafrost refers to permafrost that forms subsequent to deposition of the host sediment and rock. By contrast, syngenetic permafrost refers to permafrost that forms at the same time as the host sediment is being laid down. These types of permafrost can be distinguished by analysis of cryostructures. The epigenetic-syngenetic distinction is extremely useful in the context of Quaternary paleo-environmental reconstruction.

Cryostratigraphy adopts many of the principles of modern sedimentology. For example, 'cryofacies' are defined according to volumetric ice content and ice-crystal size, and then subdivided according to cryostructure. Finally where a number of cryofacies form a distinctive cryostratigraphic unit, these are termed a 'cryofacies assemblage' (French 2007).

(i) Cryostructures

Russian permafrost scientists were the first to systematically identify cryotextures and cryostructures (Gasanov 1963, Katasonov 1969, Zhestkova 1982, Popov et al. 1985, Melnikov & Spesivtsev 2000). Unfortunately, these classifications are complex and unwieldy. For example, Katasonov's (1969) classification lists 18 different cryostructures and Popov et al's (1985) classification lists 14 categories.

A simplified North American cryostructural classification by Murton & French (1994) encompasses the range of cryostructures found in permafrost (fig. 4). Several Russian terms are transliterated. All cryostructures can be recognized by the naked eye.

The common cryostructures are:

(1) 'structureless' (Sl) - refers to frozen sediment in which ice is not visible and consequently lacks a cryostructure. (This category is termed 'massive' in the Russian transliterated literature).
(2) 'lenticular' (Le) - lens-like ice bodies that are described by inclination, thickness, length, shape and relationship to adjacent cryostructures.
(3) 'layered' (La) – continuous bands of ice , sediment or a combination of both.
(4) 'regular reticulate' (R) - a regular three-dimensional net-like structure of ice veins surrounding a mud-rich block
(5) 'irregular reticulate' (Ri) – an irregular three-dimensional net-like structure of ice veins surrounding a mud-rich block.
(6) 'crustal' (Cr) - refers to the ice crust or rim around a rock clast.
(7) 'suspended' (Su) - refers to grains, aggregates and rock clasts suspended in ice. (This category is termed 'ataxitic' in the Russian transliterated literature).

Figure 5 shows examples of cryostructures typical for the tunnel.

The micro-morphology of cryostructures can be observed using an environmental scanning electron microscope (ESEM). For example, Bray et al (2006) provide examples of structureless (i.e. 'massive') and lenticular cryostructures viewed conventionally and under ESEM (fig. 6).

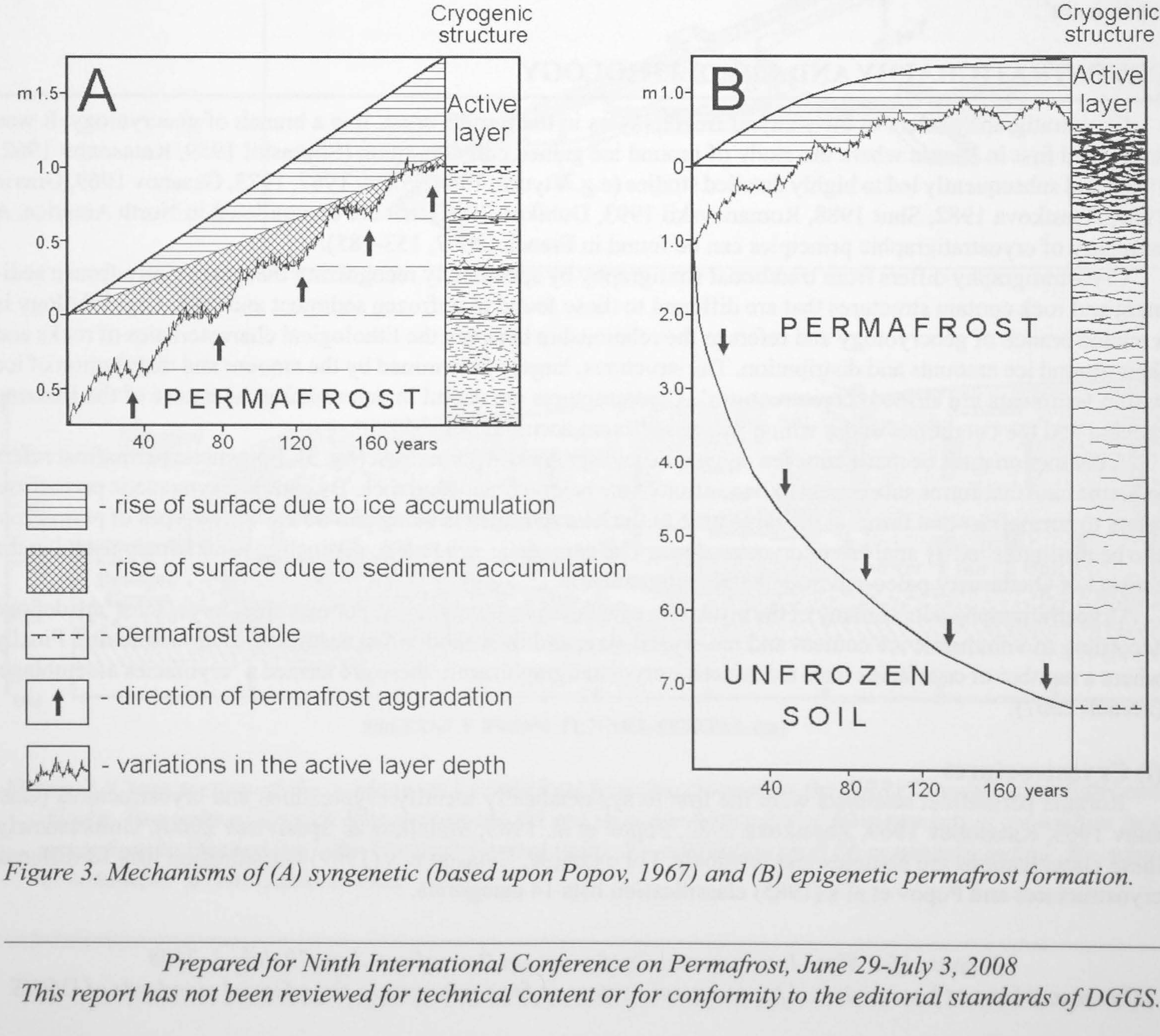

Figure 3. Mechanisms of (A) syngenetic (based upon Popov, 1967) and (B) epigenetic permafrost formation.

(ii) Thaw unconformities

Discontinuities in the nature and distribution of ground ice bodies related to permafrost thawing are termed 'thaw unconformities' (French 2007). They are the result of either thawing of frozen materials (primary thaw unconformity) or subsequent refreezing of previously-thawed material (secondary thaw unconformity). A primary thaw unconformity forms at depth below a residual thaw layer. In doing so, it truncates the top of an ice wedge. When permafrost subsequently aggrades, the original thaw unconformity at depth becomes a secondary (i.e. palaeo-) thaw unconformity and the new active layer-permafrost boundary becomes the primary thaw unconformity. The secondary thaw unconformity can be recognized by both the truncated ice wedge and by different cryostructures in the sediment above and below. Thaw unconformities can be further recognized by differences in stable isotope values, by heavy mineral assemblages above and below the unconformity, and by horizons of enhanced micro-organisms.

The manner in which permafrost degrades and subsequently forms again, and the cryostratigraphic evidence that it leaves, is illustrated in figure 7.

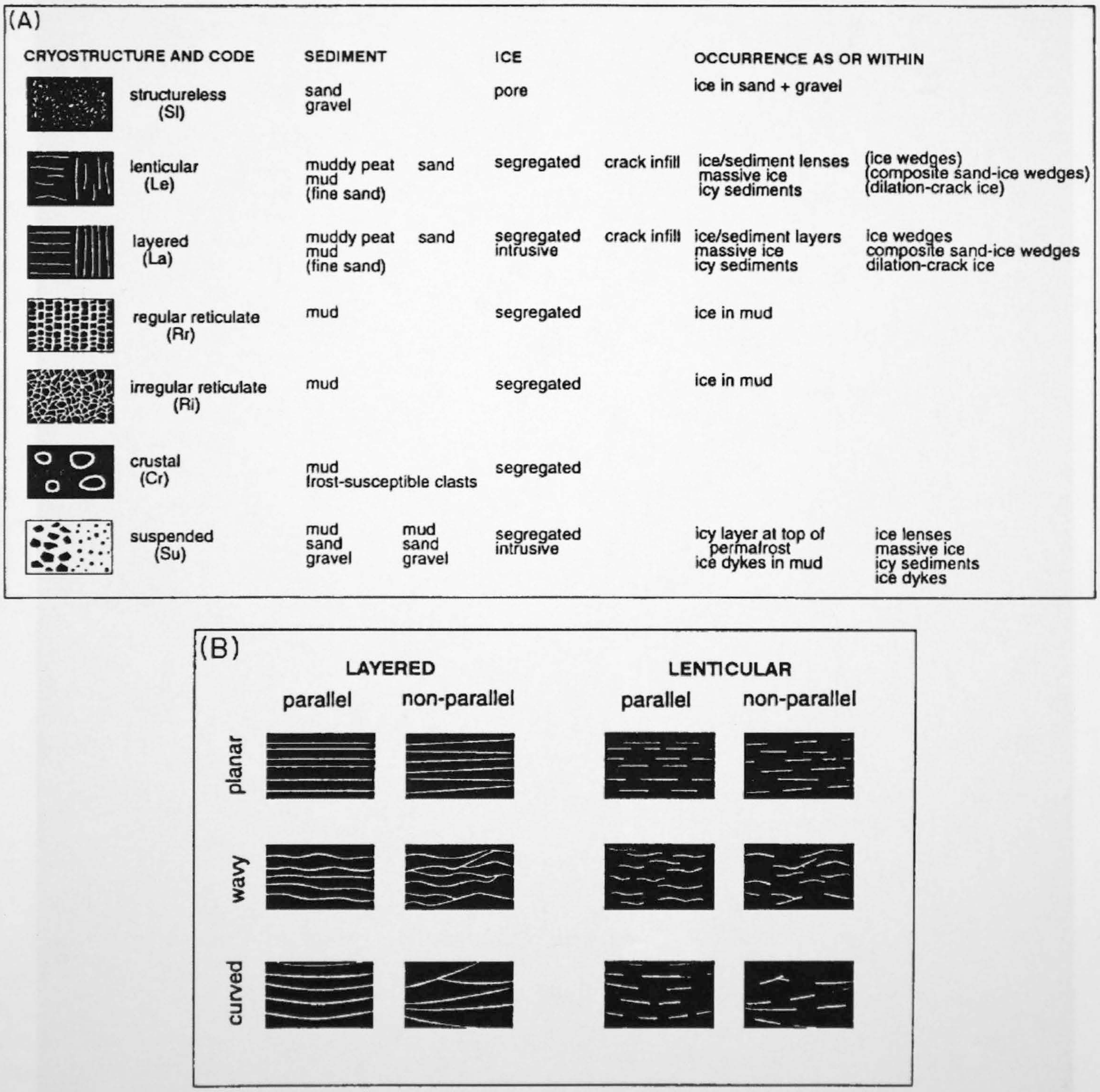

Figure 4. A North American classification of cryostructures. (A) Scheme proposed by Murton & French (1994). Ice is shown in white and sediment in black. (B) Terms and illustrations used to describe layered and lenticular cryostructures. (From Murton & French, 1994).

Figure 5. Photos showing (A) micro-lenticular cryostructure, location marker is 1.25 X 1.25 cm in size (photo by M. Kanevskiy), and (B) reticulate chaotic cryostructure, the handle of the knife is about 6 cm long (From Fortier et al. 2008).

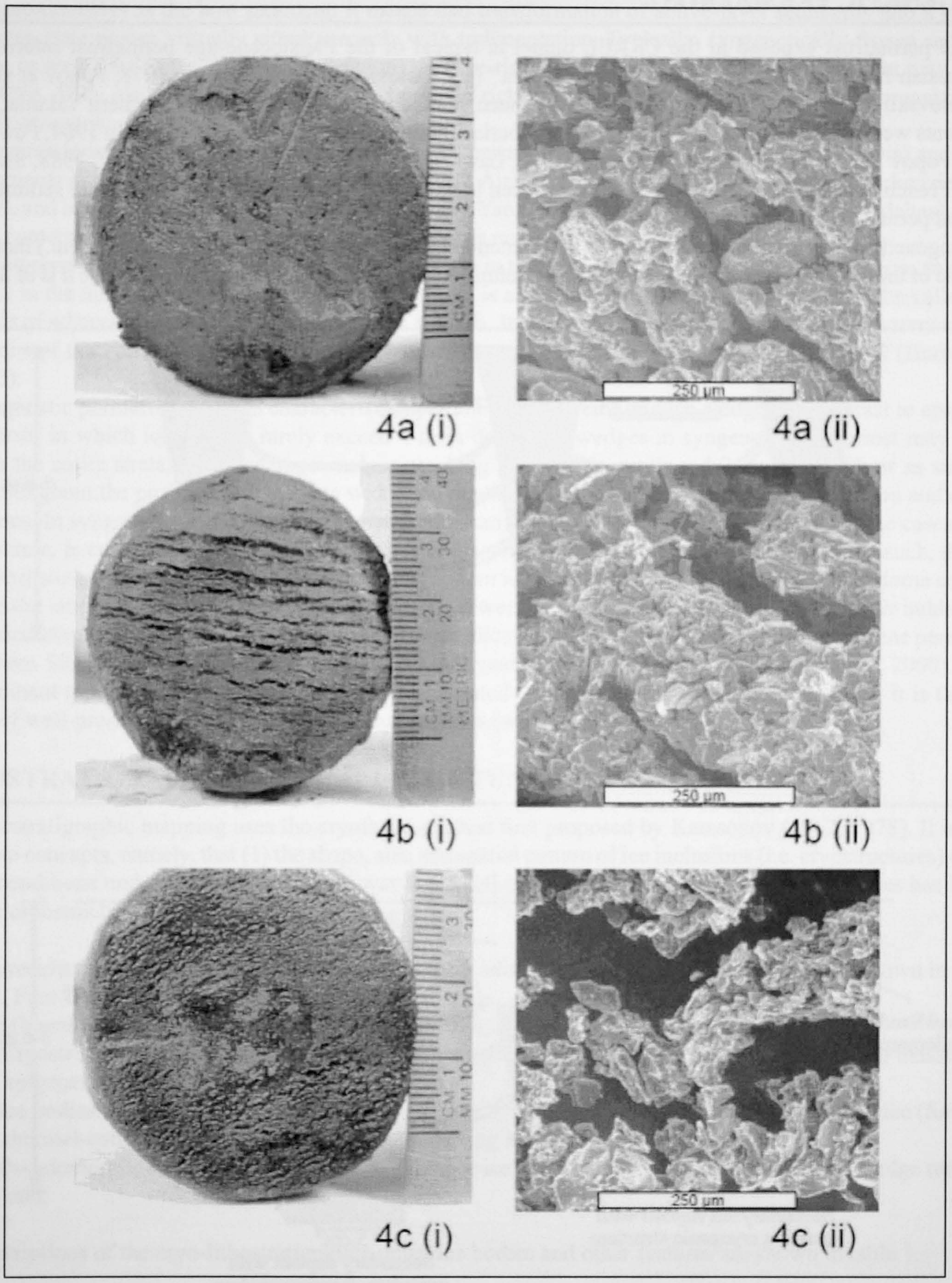

Figure 6. Example of cryostructures from the CRREL tunnel viewed conventionally and under ESEM. (a) Massive cryostructure. Image (i) is a macro-scale image typical of silt pseudomorphs. Note centimeter scale. Image (ii) is a micro-scale image using an ESEM. Bar scale indicates 250 mm. (b) Lenticular-layered cryostructure. Image (i) is a conventional macro-scale image. Note centimeter scale. Image (ii) is a micro-scale image using an ESEM that shows the soil and micro ice-lens morphology. Bar scale indicates 250 mm. (c) Micro-lenticular cryostructure. Image (i) is a macro-scale image. Note centimeter scale. Image (ii) is a micro-scale images under ESEM in which soil particles are generally suspended in an ice matrix. Bar scale indicates 250 mm. (From Bray et al 2006).

SYNGENETIC PERMAFROST

The permafrost exposed in the CRREL tunnel is typical of the Pleistocene-age permafrost referred to in the Russian literature as "Yedoma" or "Ice Complex" (e.g. Soloviev 1959, Katasonov 1978, Popov et al. 1985, Romanovskii 1993). Ice Complex sediments have been studied mainly in Central and Northern Yakutia; similar sediments were observed also in Chukotka, West Siberia, Taimyr, Alaska, and Canada (Vtyurin 1964, Péwé 1966, 1975, Popov 1967, Gasanov 1969, Katasonov 1978, Lawson 1983, Carter 1988, Hamilton et al. 1988, Shur et al. 2004, French 2007). This permafrost developed when long periods of uninterrupted cold-climate sedimentation allowed permafrost to form syngenetically.

Syngenetic permafrost forms in response to sedimentation (alluvial, slope, aeolian, lacustrine, etc.) that causes the base of the active layer to aggrade upwards. By definition, the permafrost is syngenetic because it is of the same

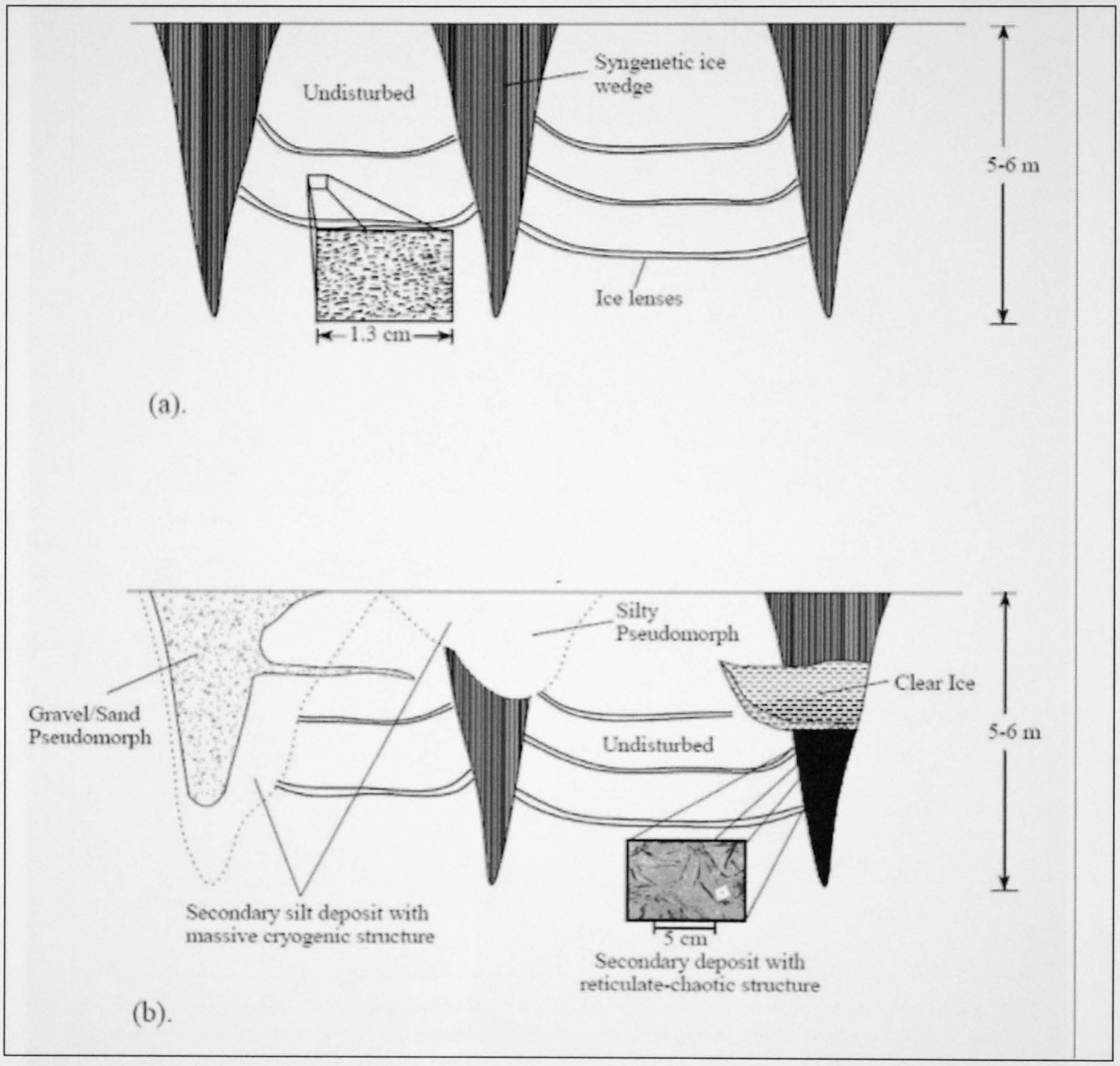

Figure 7. Schematic diagram of (a) undisturbed syngenetic permafrost and (b) typical modified permafrost exposure within the CRREL tunnel. In (a) the expanded image represents a micro-lenticular cryostructure, a reliable indicator of syngenetic permafrost. In (b) an idealized schematic shows typical secondary modification of original syngenetic permafrost. Expanded image represents reticulate-chaotic cryostructures. The reticulate-chaotic cryostructure is associated with 'clear ice', interpreted as thermokarst-cave ('pool') ice. (From Bray et al. 2006).

age (approximately) as the host sediment. It means that transformation of active-layer sediments into a perennially-frozen state occurs virtually simultaneously with sedimentation. Typically, syngenetically-frozen sediments are silty, or loess-like (up to 70-80% silt fraction), and ice-rich (the soil gravimetric moisture content may exceed 100-200%). They also contain rootlets, buried organic-rich horizons, and exhibit rhythmically-organized (i.e. layered) cryogenic structures.

The main locations where contemporary syngenetic permafrost is forming today are in the alluvial and deltaic environments (Shur & Jorgenson 1999) of Arctic North America (e.g. Colville River, Alaska; Mackenzie River, Canada), and in northern Siberia (e.g. Lena, Ob, Yenisey, Yana, Indigirka, Kolyma river valleys and deltas). Thickness of contemporary syngenetic permafrost usually does not exceed a few meters.

Pleistocene-age syngenetic permafrost occurs mainly in the continuous permafrost zone of Siberia, and its occurrence in the discontinuous permafrost zone of Alaska is a rare phenomenon. It is also found in the valleys and lowlands of adjacent unglaciated Yukon Territory, Canada. It should be mentioned that, under the current climatic conditions of the Fairbanks area, modern ice-wedge formation occurs very rarely and only in peat (Hamilton et al. 1983).

Syngenetic permafrost is often characterized by numerous ice veins and ice wedges. In contrast to epigenetic permafrost, in which ice wedges rarely exceed 4 m in depth, ice wedges in syngenetic permafrost may extend through the entire strata, either as huge wedges reaching 10-40 m in depth and 2-6 m in width or as small ice veins throughout the profile. Their varying width and depth reflect the varying rates of sedimentation and climate conditions. In syngenetic permafrost bodies, wedge ice can occupy 30-50%, and even more in some cases, of the total volume. In color, the wedges are grey because of the numerous inclusions of fine sediment. As such, they can easily be distinguished from smaller Holocene and modern ice wedges located in the top part of Yedoma sections, because the latter are usually white and opaque due to fewer soil inclusions and an abundance of air bubbles.

Radiocarbon dating and oxygen-isotope variations indicate that much of the syngenetic Pleistocene permafrost in northern Siberia formed between 40,000 and 12,000 years ago (Vasil'chuk & Vasil'chuk 1997, 2000). It was the dominant type of permafrost that formed in unglaciated lowlands during the Late Pleistocene. It is the main source of well-preserved Late-Pleistocene faunal remains (woolly mammoths etc).

CRYOSTRATIGRAPHIC MAPPING IN THE TUNNEL

Cryostratigraphic mapping uses the cryofacial method first proposed by Katasonov (1962, 1978). It is based upon two concepts, namely, that (1) the shape, size and spatial pattern of ice inclusions (i.e. cryostructures) depend on the conditions under which the sediment was deposited and then frozen, and (2) every cryofacies has its own specific cryostructure.

The results of cryostratigraphic mapping of the main adit of the tunnel (Bray et al. 2006) are shown in figures 8 and 9. Four categories of information are shown:

(a) Mineral sediment is grouped into the general categories of silt, sand and gravel.

(b) Cryostructures are identified as being either lenticular or micro-lenticular (i.e. syngenetic), massive (i.e. epigenetic) or reticulate-chaotic (i.e. epigenetic).

(c) Ice bodies are mapped as being either lenses (usually a layered cryogenic structure), wedge ice (formed in thermal-contraction cracks), or clear ice (occurring in association with wedge ice).

(d) Pseudomorphs are mapped where the sediment or ice is interpreted to be the result of ice-wedge modification.

Descriptions of the cryo-lithostratigraphic units, ice bodies and other features are shown in table 1.

In 2006, the 38 m long winze section was studied (Kanevskiy et al. 2008). Cryostratigraphic mapping of one wall and the ceiling of the winze was performed in the scale 1:20; several small sections were studied in detail (scale 1:4). Figure 10 shows the general view of the left wall and the ceiling of the winze. More detailed fragments are shown in figures 11 to 13.

CRYOSTRUCTURES

Recent publications (Shur et al. 2004, Bray et al. 2006, Fortier et al. 2008, Kanevskiy et al. 2008) show the variety of cryostructures that are present in the tunnel and describe typical features related to syngenetic permafrost formation.

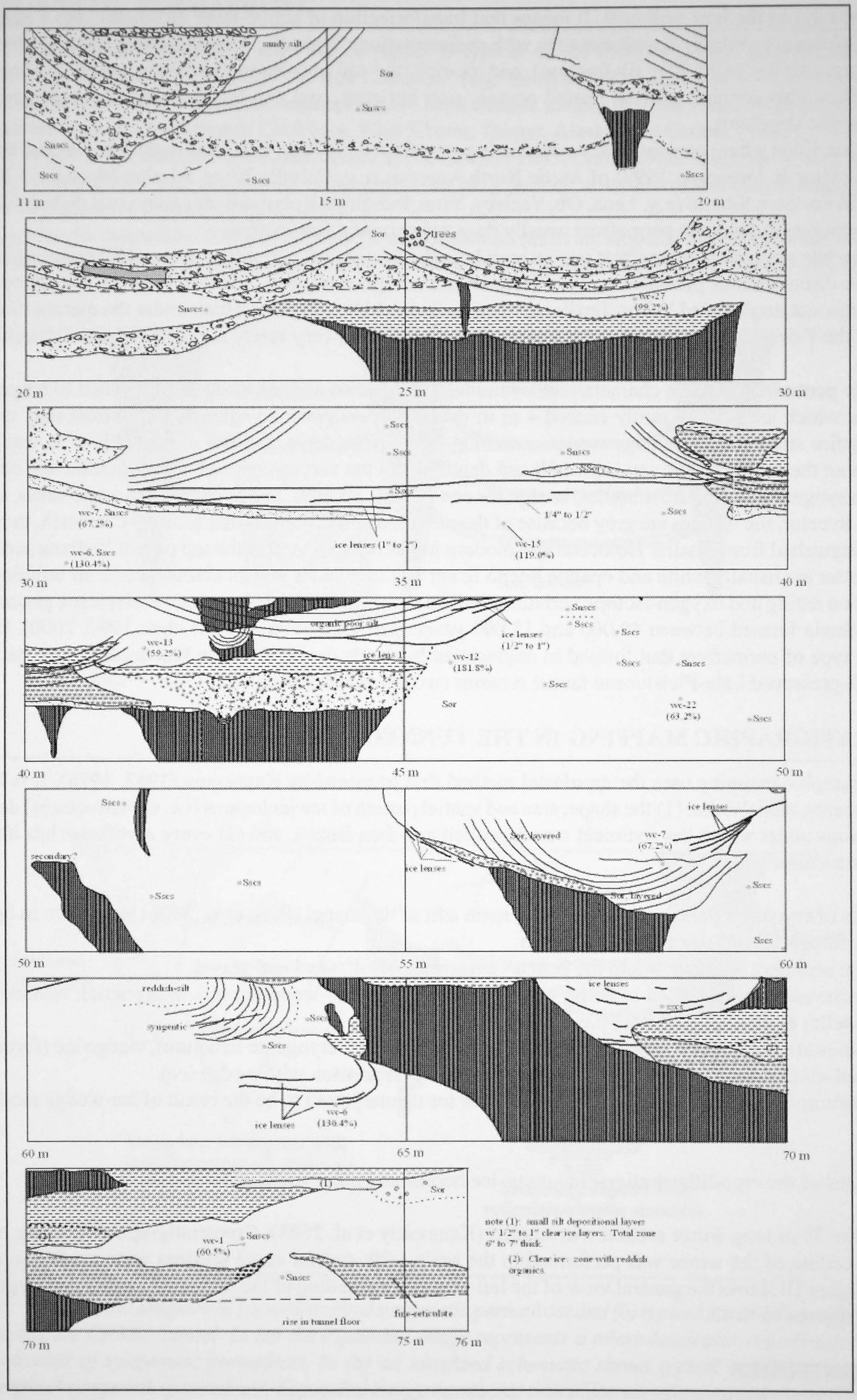

Figure 8. Cryostratigraphic map of part of the main shaft of the CRREL Permafrost Tunnel, left side (viewed from entrance) of the tunnel. For the legend, see Figure 9. (From Bray et al. 2006).

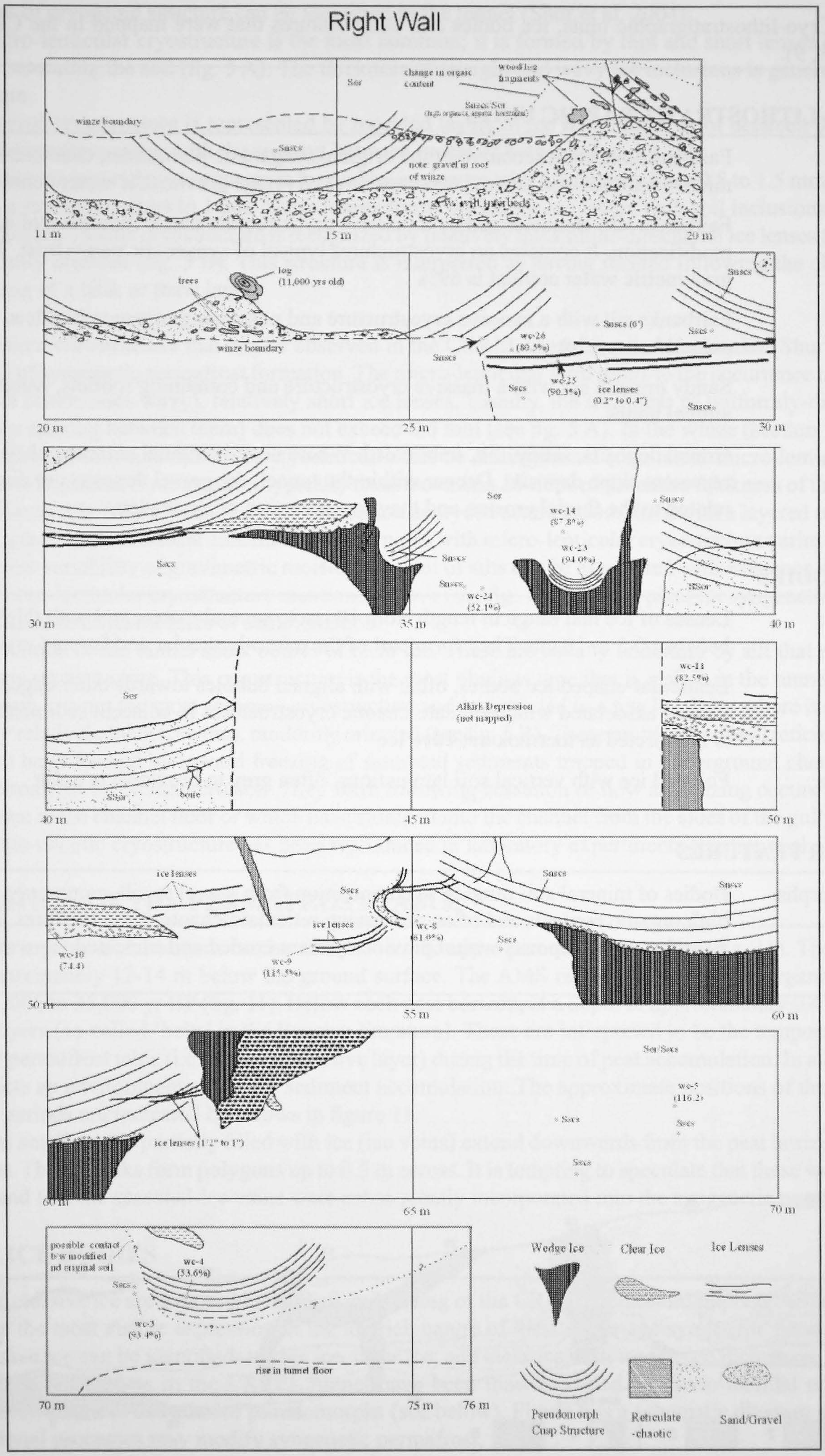

Figure 9. Cryostratigraphic map of part of the main shaft of the CRREL Permafrost Tunnel, right side (viewed from entrance) of the tunnel. (From Bray et al. 2006).

Table 1. Cryo-lithostratigraphic units, ice bodies and other features that were mapped in the CRREL tunnel (see figs. 8, 9).

1. CRYO-LITHOSTRATIGRAPHIC UNITS

Sscs:	Fairbanks silt, representative of the original syngenetic permafrost, characterized by micro-lenticular and layered cryostructures. Average gravimetric water content 130%
Snscs:	Fairbanks silt, characterized by a massive cryostructure that is indicative of secondary modification. It contains no cryostructures typical of syngenetic permafrost. The average gravimetric water content is 69%
Sor:	Fairbanks silt with a massive cryostructure and possessing organics (rootlets, wood, animal bones, etc)
Ssor:	Sandy organic silt with a massive cryostructure and containing rootlets, wood and animal bones
Gr:	Gravel deposits; sandy, silt, imbricated. Where near the tunnel entrance, they may represent slope deposits. Deeper within the tunnel, the gravel deposits are directly related to the fluvial erosion and thaw-modification of ice wedges

2. ICE BODIES

Ice lenses:	Lenses of ice that range in length from 10 cm to several meters and with thickness of between 0.5 to 10 cm. They form part of the micro-lenticular and layered cryostructures
Clear ice:	Lenticular-shaped ice bodies, often with aligned bubbles towards outer edges, and usually associated with reticulate-chaotic cryostructures in adjacent sediments. The ice is interpreted as thermokarst-cave ice
Wedge ice:	Foliated ice with vertical soil laminations, often grey to brownish in color

3. OTHER FEATURES

Pseudomorphs:	Bodies of mineral soil ranging in composition from gravel to silt, commonly possessing high organic contents and often possessing reticulate-chaotic cryostructures. Interpreted as replacement deposits within previously thaw-eroded and truncated ice-wedge structures

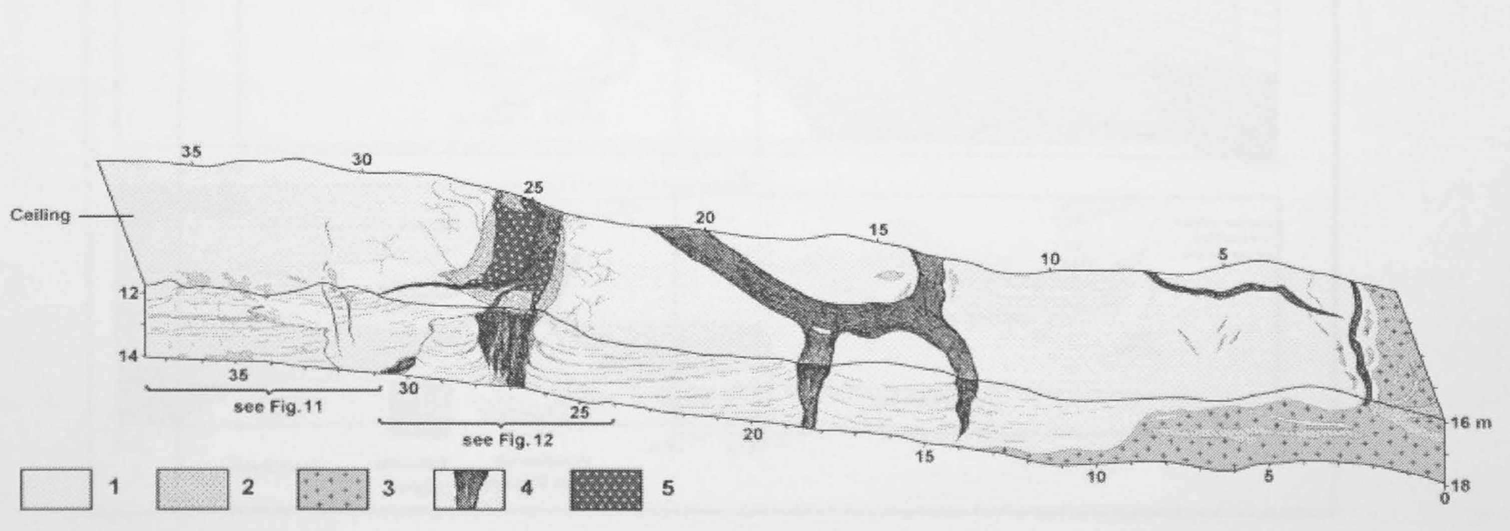

Figure 10. General view of the left wall and the ceiling of the winze. 1 – silt; 2 – sand; 3 – Fox Gravel; 4 – ice wedge; 5 – thermokarst-cave ice. See figures 11 to 13 for details. (From Kanevskiy et al. 2008).

Four types of cryogenic structure can be identified in the tunnel (Shur et al. 2004):

(1) A micro-lenticular cryostructure is the most common; it is formed by thin and short lenses of ice practically saturating the soil (fig. 5 A). The thickness of straight and wavy ice inclusions is generally less than 0.5 mm.

(2) A layered cryostructure is represented by repeated layers of ice with thickness of between 0.2 and 1 cm. The layers form series with the spacing between layers of between 2 and 5 cm.

(3) A lenticular-layered cryostructure is formed by ice lenses with a thickness from 0.5 to 1.5 mm and a length from a few millimeters to 1 cm. These lenses form continuous ice layers with soil inclusions.

(4) A reticulate-chaotic cryostructure is recognized by relatively thick multi-directional ice lenses (veins), often randomly oriented (fig. 5 B). This structure is interpreted as having formed following the closed-system freezing of a tálik or thaw layer.

The dominant cryostructure that can be observed in the CRREL tunnel is micro-lenticular (Shur et al. 2004). This is typical of syngenetic permafrost formation. The micro-lenticular term refers to the occurrence of very small, sub-horizontal (sometimes wavy), relatively short ice lenses. Usually, the thickness of uniformly-distributed ice lenses (and the spacing between them) does not exceed 0.5 mm (see fig. 5 A). In the winze (section 1, see fig. 13 A), several varieties of micro-lenticular cryostructure can be distinguished (e.g. latent micro-lenticular, micro-braided). Micro-lenticular cryostructures typically form more than 50-60% of the entire thickness of the syngenetic permafrost (Kanevskiy 2003). Usually the micro-lenticular cryostructure is combined with a layered cryostructure. In the tunnel, gravimetric moisture content of the sediments with micro-lenticular cryostructure varies from 80% to 240%. The great variability of gravimetric moisture content of silts can be associated with existence of the several varieties of micro-lenticular cryostructure mentioned above (see fig. 13 A). It is typical for syngenetic permafrost, and mostly linked to different rates of sedimentation.

Certain sections of the tunnel show bodies of clear ice. These are usually underlain by silt that exhibits a reticulate-chaotic cryostructure. This cryostructure is the most obvious type that is visible in the tunnel (Shur et al. 2004). However, it is not the most common cryostructure and is restricted to a few localities where it can be easily recognized by relatively thick ice veins, randomly oriented (see fig. 5 B). These multi-directional reticulate ice veins are thought to have formed by inward freezing of saturated sediments trapped in underground channels incised within the permafrost by thermal erosion. They form following cessation of flow as freezing occurs in sediments either laid down in the channel floor or which have slumped into the channel from the sides of the gully. Formation of the reticulate-chaotic cryostructure has been reproduced in laboratory experiments (Fortier et al. 2008).

AGGRADATION OF THE PERMAFROST TABLE

Seven thin organic-rich horizons can be observed in the upper part of the winze (see fig. 11). They occur at a depth of approximately 12-14 m below the ground surface. The AMS radiocarbon dates for organic-rich layers vary from 31,000 to 35,000 yr BP (fig. 11). Below each peat horizon, at a depth of approximately 0.4 to 0.6 m, are distinct icy layers (so-called 'belts' in the Russian literature). These are interpreted to be the temporary positions of the former permafrost table (i.e. base of the active layer) during the time of peat accumulation. In all probability, the peat reflects an environment of slower sediment accumulation. The approximate positions of the active layer during these periods are indicated by arrows in figure 11.

Numerous small cracks partially filled with ice (ice veins) extend downwards from the peat horizons to depths of up to 0.5 m. These cracks form polygons up to 0.5 m across. It is tempting to speculate that these were seasonal-frost cracks and that the seasonal-ice veins were subsequently incorporated into the syngenetic permafrost.

MASSIVE ICE BODIES

Bodies of massive ice are exposed in the wall and ceiling of the CRREL tunnel and impress the first-time visitor. These are the most visible expression of the ice-rich nature of Pleistocene-age syngenetic permafrost. Three types of massive ice can be identified: wedge ice, clear ice, and clear ice with wedge-ice inclusions.

Many of the ice wedges in the CRREL tunnel have been thaw-modified by fluvio-thermal erosion which promotes the formation of soil and ice pseudomorphs (see below). Figure 6 is a schematic diagram showing how thermal erosional processes may modify syngenetic permafrost.

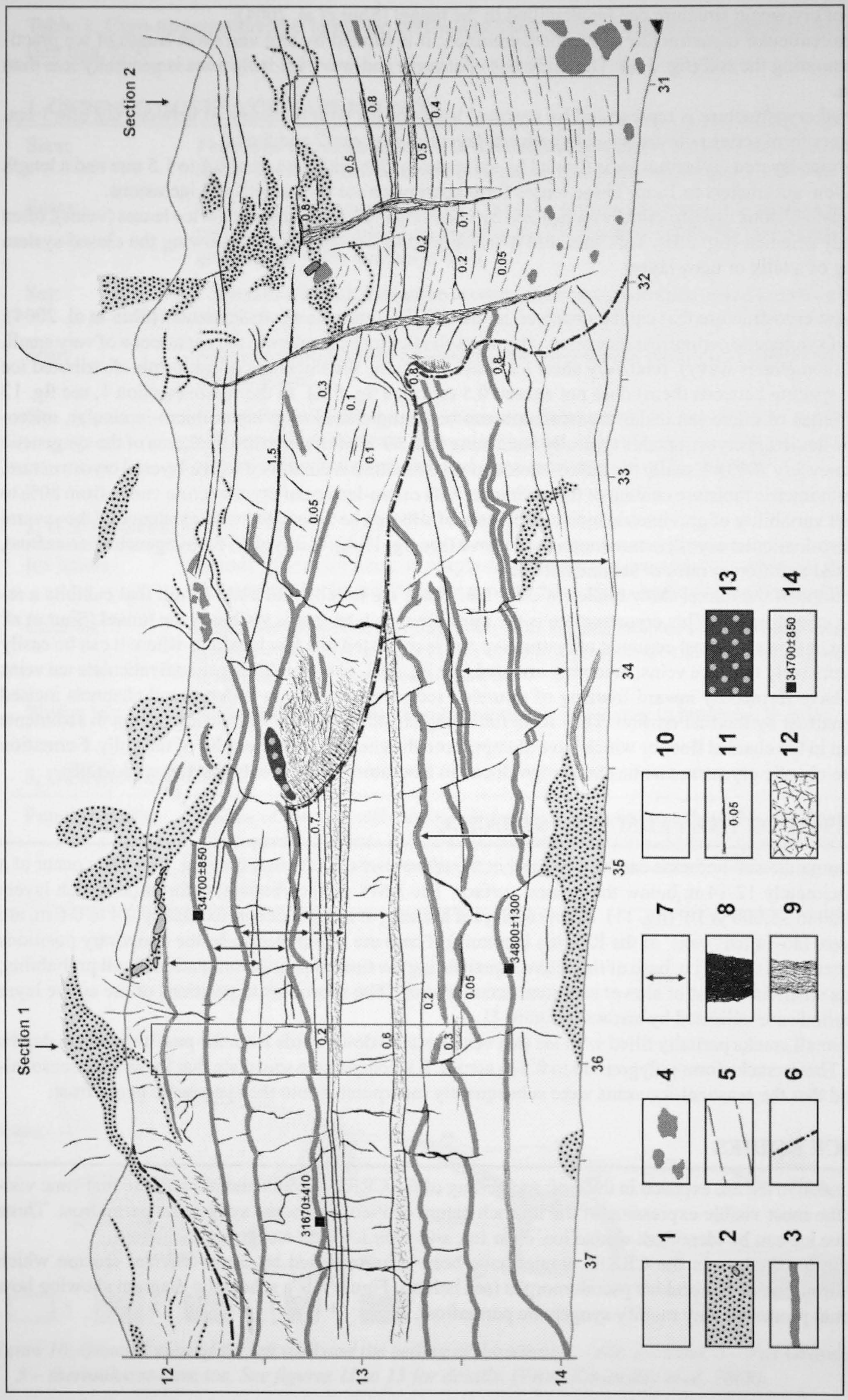

Figure 11. Cryostratigraphic map of the left wall of the winze, interval 31-37 m. 1 – silt; 2 – sand, gravel inclusion; 3 – in situ peat layers; 4 – inclusions of re-transported organic matter; 5 – lamination in silt; 6 – erosion boundary; 7 – approximate position of active layer at the periods of slower sedimentation; 8 – ice wedge; 9 – composite wedge (ice/silt); 10 – isolated ice vein; 11 – ice layer ('belt'), thickness in cm; 12 – reticulate-chaotic cryostructure; 13 – thermokarst-cave ice; 14 – radiocarbon date, yr BP. (From Kanevskiy et al. 2008).

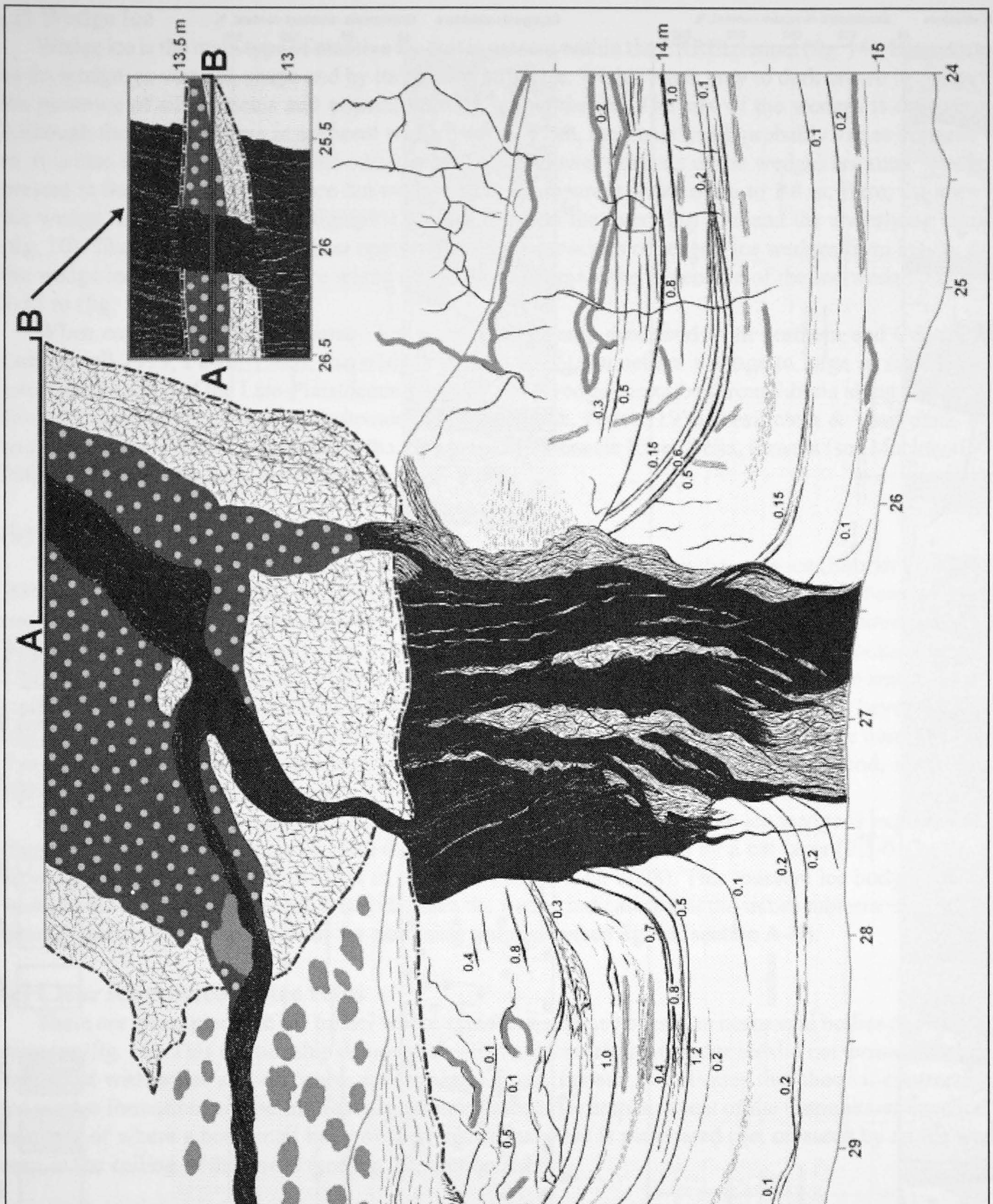

Figure 12. Cryostratigraphic map of the left wall of the winze, interval 24-31 m. For the legend, see Figure 11. A-B – schematic reconstruction of vertical section through the ice pseudomorph, located at the ceiling of the winze. (From Kanevsky et al. 2008).

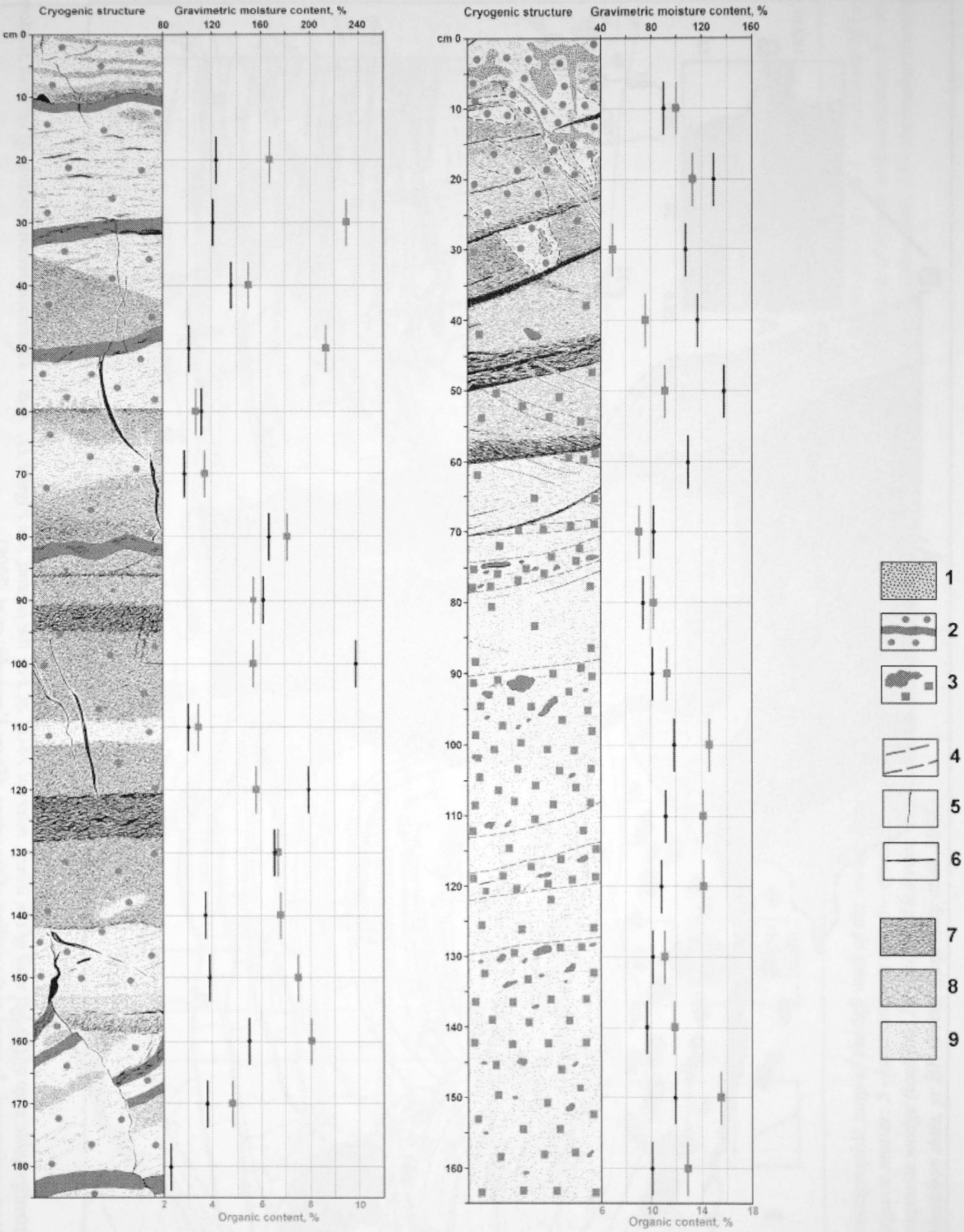

Figure 13. Details of cryogenic structure and properties of sections #1 (a) and #2 (b); location of sections is shown at Figure 11. 1 – sand; 2 – in situ peat layer and inclusions of organic matter; 3 – inclusions of retransported organic matter; 4 – lamination in silt; 5 – isolated ice vein; 6 – distinct ice layer ('belt'); 7 – micro-braided cryostructure; 8 – micro-lenticular cryostructure; 9 – latent micro-lenticular / porous cryostructure. (From Kanevskiy et al. 2008).

(a) Wedge ice

Wedge ice is the main type of massive ice that is present within the CRREL tunnel (fig. 14). It is easy to recognize by its wedge, or vertical, shape and by its foliated structure. Wedge ice is grey to dark brown in color; this reflects the presence of silt particles and organic staining within the ice. The size of the wedges is difficult to quantify. Although the wedges range in apparent width from 1 to 7 m, their true width probably varies between 0.5 and 3.0 m. It is also important to stress that only the middle and lower portions of the wedges are seen. Wedge ice is also present in the winze section where the wedges have an apparent width of up to 1.8 m. Here, the apex (nipple) of the wedge terminates at the stratigraphic contact between the overlying silts and the underlying alluvial gravels (fig. 10). The tunnel presents a great opportunity to see crossings of several ice wedges from inside: exposures of the wedge ice in the ceiling of the winze allow one to estimate the dimension of the ice-wedge polygons to reach 8-12 m (fig. 10).

When compared to the epigenetic ice wedges commonly described from northern and Central Alaska (e.g. Leffingwell 1919, Péwé, 1966), the wedges in the CRREL tunnel are average to large in size. However, when compared to some of the Late-Pleistocene syngenetic ice wedges described from Siberia along the Yana or Kolyma Rivers in northern Siberia (see Dostovalov & Popov 1966, Popov, 1973, Vasil'chuk & Vasil'chuk 1997), or the anti-syngenetic wedges inferred from the Pleistocene Mackenzie River Delta, Canada (see Mackay, 1995; French, 2007, 181), they appear to be average to small in size.

(b) Clear ice

We interpret the clear ice bodies in the CRREL tunnel to be thermokarst-cave ice (Shur et al. 2004, Bray et al. 2006). In North America, this is known colloquially as 'pool' ice (Mackay 1997). This is because ice-rich syngenetic permafrost is highly susceptible to thermal erosion that promotes the formation of subterra¬nean channels. When these channels are finally closed by sediment, water that is ponded behind the blockage begins to freeze. This process results in formation of thermokarst-¬cave ('pool') ice. The clear ice bodies are lenticular shaped. Their visible thickness in the tunnel ranges from a few centimeters to about 2 m and their extent beyond the ceiling is not known. The largest apparent horizontal extent of this type of ice that can be viewed in the tunnel is approximately 7 m. The alternative interpretation, that these clear ice bodies are buried surface, or pond, ice (Sellmann 1967, Hamilton et al. 1988), is not supported by the cryostructures present in the tunnel.

In the winze, a horizontal body of thermokarst-cave ice crosscutting the ice wedge is exposed on the ceiling (figs. 12, 14). Its thickness varies from 0.2 to 0.35 m and it is underlain by a silt layer (0.1-0.4 m thick) having a reticulate-chaotic cryostructure (Shur et al. 2004, Fortier et al. 2008). This massive ice body is aligned with the width of the ice wedge; however, it is wider than the wedge indicating that the initial subterra¬nean channel eroded laterally across the ice wedge into the enclosing sediments (see fig. 11, section A-B).

(c) Clear ice crossed by ice veins

There are many places in the tunnel where veins of wedge ice penetrate horizontal bodies of clear thermokarst-cave ice (fig. 15). This relationship demonstrates that the formation of wedge ice did not terminate when the cavity was filled with water and the water subsequently froze. Instead, it indicates that thermal-contraction cracking, ice-wedge formation, and permafrost growth continued after emplacement of the thermokarst-cave ice. The other example of where a horizontal body of thermokarst-cave ice is penetrated (i.e. crossed) by an ice wedge can be seen in the ceiling of the winze (see fig. 12, section A-B).

THERMAL EROSION, SOIL AND ICE PSEUDOMORPHS

Numerous sites of former gullies and underground channels can be observed in the silty sediments at various depths. They appear to have been cut by running water and afterwards filled with thermokarst-cave ice and soil whose structure and properties differ from the original syngenetic permafrost (Shur et al. 2004, Bray et al. 2006, Fortier et al. 2008).

The formation of thermokarst-cave ice is related to the gully erosion that must have occurred, especially during the spring snowmelt, during growth of the syngenetic permafrost on the relatively gently-sloping terrain of Goldstream Valley where the CRREL tunnel is located (Shur et al. 2004). It is necessary to stress that syngenetic permafrost, composed predominantly of ice-rich silty sediments, is especially susceptible to fluvio-thermal erosion (Shur et al. 2004, Bray et al. 2006, Fortier et al. 2007). Fluvio-thermal erosion occurs when surface runoff, from snowmelt, summer precipitation or thawing permafrost, becomes concentrated mainly along ice wedges causing preferential thaw. The gullies that result frequently assume an inverted 'T' cross-profile because water first erodes

Figure 14. Photo showing ice wedge dissecting a horizontal lens of white thermokarst-cave ice (ice pseudomorph), right wall of the winze. The width of the wedge is 1.0 m. The thermokarst-cave ice body is underlain by several silt layers with reticulate-chaotic cryostructure. The same wedge exposed on the opposite wall of the winze is shown in Figure 12. (Photo by M. Kanevskiy).

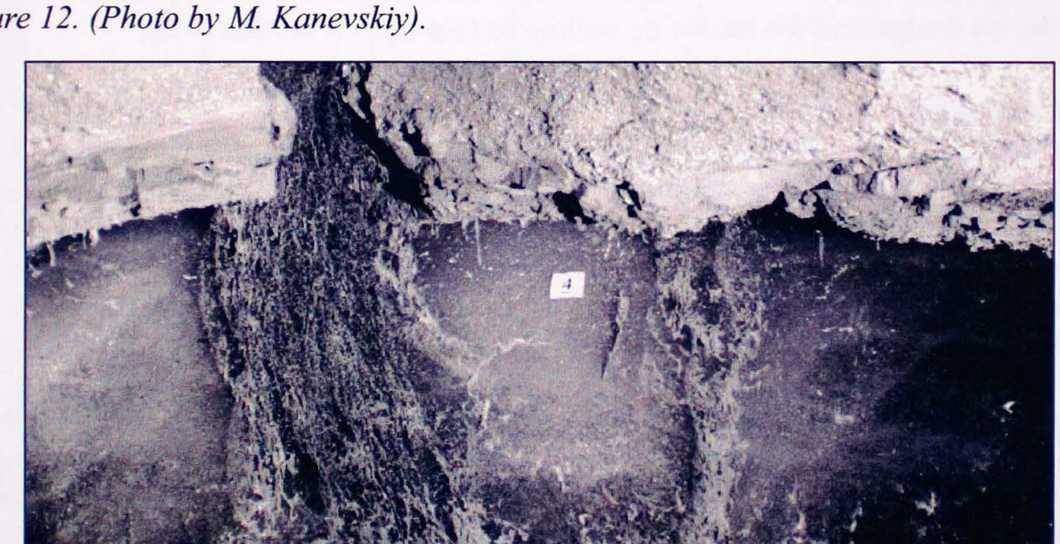

Figure 15. Photo showing veins of wedge ice penetrating a near-horizontal layer of thermokarst-cave ice. The location marker is 2.5 X 2.5 cm in size. (From Shur et al. 2004).

vertically and then, as the bed becomes armored with transported sediment from up-gully, laterally. This often leaves an organic-mat overhang. Slumping, piping and the creation of small tunnels above and adjacent to the partially-eroded ice wedge are also common. Fluvio-thermal erosion and the thaw-modification of ice wedges is a well known process in Arctic regions today (see French 2007, 191-2; Fortier et al. 2007). What is less well known is that, sometimes, standing water bodies accumulate in the channel floor behind slumped masses to form the ice bodies that Shumskii (1959) termed 'thermokarst-cave ice'.

The formation of pseudomorphs is related to the thaw-modification of ice wedges that would have occurred also during fluvio-thermal or underground-erosion episodes. Soil pseudomorphs are formed by silt or gravel filling the void left by the eroded ice wedge; ice pseudomorphs are formed by thermokarst-cave ice filling the void (fig. 6). These structures represent secondary infilling. Ice, sediment or an ice-sediment mix constitutes the infill. It is not surprising that the cryogenic properties of this infill material differ from the enclosing syngenetic permafrost. Formation of these structures is regarded as typical of syngenetic permafrost growth.

Both types of pseudomorphs (soil and ice) exist in the CRREL tunnel. However, they are difficult to recognize, especially ice pseudomorphs, because some have been subsequently modified by the penetration of ice veins. The incorporation of ice veins into ice pseudomorphs demonstrates that the formation of wedge ice is not terminated by the formation of thermokarst-cave ice (Shur et al. 2004). An ice pseudomorph modified by the penetration of ice veins is shown in figure 15.

Recent examination of the main adit showed that, of 20 ice wedges identified, 19 had been subject to thermal erosion. Approximately 60% of the channels cutting through the ice wedges and the enclosing syngenetic permafrost were partially or entirely filled by thermokarst-cave ice (Fortier et al. 2008).

In the winze, a gully filled with sediments can be observed at interval 29-35 m (see figs. 10 to 13). A truncated ice wedge affected by thermal erosion is located under this gully. The sediments filling the gully are mostly ice-poor stratified silts with lenses of sands. They contain numerous inclusions of organic material, which are interpreted as having been reworked by water. The organic content of the sediments in the gully varies from 7.0% to 22.8% by weight and is much higher in comparison with the original permafrost (Section 2, fig. 13 B).

Cryostructures in the lower part of section 2 (fig. 13 B, 60-165 cm) vary from latent micro-lenticular to porous (structureless). The gravimetric moisture content of this part of section 2 varies from 70% to 100% which is smaller than the water content of the original syngenetic permafrost. Such water content is unusual for sediments with very small amount of visible ice. It can be attributed to the higher organic content (fig. 13 B). Sediments with an organic content of 9-12% have a gravimetric moisture content of 70-80%, whereas sediments with organic content of 14-16% have a moisture content of 90-100%. The cryostructures and ice contents of the upper part of the section 2 (fig. 13 B, 0-60 cm) are similar to those of the original permafrost; here, the gravimetric moisture contents vary from 110% to 140%. This indicates change of sedimentation mode and decrease of sedimentation rate at the last stages of gully infilling.

ICE CONTENT

The ice content of sediments exposed in the tunnel varies widely. Although the weathered schist exposed in the lowest part of the Gravel Room contains a very small amount of visible ice, its gravimetric moisture content varies from 6.5% to 19.9%, averaging 11.7% (Hamilton et al. 1988). Gravimetric moisture content of alluvial gravel exposed in the lowest part of the winze generally is 8.9% to 10.3% (Hamilton et al. 1988). Typically, the gravel contains crustal cryostructures with thin ice crusts enclosing the gravel clasts. Close to the contact with overlying silt the thickness of ice crusts increases: sometimes it can reach 0.5-2.0 cm. Silt is generally ice-rich: gravimetric moisture content varies from 39% to 139% (Hamilton et al. 1988).

Recent studies show that the ice content of silt strongly depends on its cryostructure. For sediments with micro-lenticular cryostructure, gravimetric moisture content in the main adit varies from 80% to 180%, averaging 130% (Bray et al. 2006). A similar range (100-240%) is found in the winze (Section 1, fig. 13 A). For modified sediments with structureless (or massive) cryostructure, which fill gullies and soil pseudomorphs, gravimetric moisture content in the main adit varies from 50% to 95%, averaging 69% (Bray et al. 2006). For similar sediments in the winze, gravimetric moisture content is 70-100% (section 2, fig. 13 B, 60-165 cm). We associate the unusually high moisture content of ice-poor silt with the high content of reworked organic material in these sediments. The average gravimetric moisture content of the cross-stratified sands with structureless (or massive) cryostructure, filling underground channels, is 44.6%, whereas it is 107.7% in the surrounding permafrost with micro-lenticular cryostructure (Fortier et al. 2008). For sediments with reticulate-chaotic cryostructure, gravimetric moisture content in the main adit varies from 60% to 115%, averaging 85% (Bray et al. 2006).

TWO SILT UNITS?

The early studies in the tunnel (Sellmann 1967, 1972, Hamilton et al. 1988) did not adequately recognize the syngenetic nature of the permafrost. Two independent systems of ice wedges and an inferred thaw unconformity that separated the silts into an upper and a lower unit were recognized (see fig. 2). Some ice bodies, described as '...horizontal, saucer-shaped bodies' were interpreted as buried frozen thaw ponds formed in ice-wedge troughs, are better explained as bodies of thermokarst-cave ('pool') ice formed in underground channels.

There is now evidence that thermal-erosion processes were simultaneous with permafrost formation. First, the clear ice bodies are best explained as thermokarst-cave ice. Second, the occurrence of ice veins that penetrate thermokarst-cave ice means that ice wedges continued to grow after their partial thaw-modification and destruction by fluvio-thermal erosion and the subsequent pooling of water within the erosional void. Third, the dominant cryogenic structure is similar throughout the whole silt section. Fourth, the radiocarbon ages obtained from sediments within the tunnel do not reveal any sufficient break in sedimentation. In fact, no clear evidence of regional or widespread thermokarst can be found in the tunnel; instead, the thaw unconformities appear localized and connected with previous gullies and underground channels.

In summary, the cryostratigraphic data do not confirm the existence of two silt units divided by a continuous thaw unconformity, as described previously. Cryostructures, truncated ice bodies, and soil and ice pseudomorphs suggest a single sequence of continuous sedimentation and syngenetic permafrost aggradation in Late-Pleistocene time. This permafrost has been reworked by local thermal-erosional events.

REFERENCES

Arcone, S.A. & Delaney, A.J., 1984. Field dielectric measurements of frozen silt using VHF pulses. Cold Regions Science and Technology 9: 29-37.

Bray, M.T., 2008. Effects of soils cryostructure on the long term strength of ice-rich permafrost near melting temperatures. Proceedings of the Ninth International Conference on Permafrost (in press).

Bray, M.T., French, H.M. & Shur, Y., 2006. Further cryostratigraphic observations in the CRREL permafrost tunnel, Fox, Alaska. Permafrost and Periglacial Processes 17 (3): 233-243.

Carter, L.D., 1988. Loess and deep thermokarst basins in Arctic Alaska. Proceedings of the Fifth International Conference on Permafrost. Tapir publishers, Trondheim, Norway: 706-711.

Chester, J.W., and Frank, J.N., 1969. Fairbanks Placers Fragmentation Research, Final Report. U.S. Department of Interior, Bureau of Mines, Metals Program, Auth. no. L1115-33: 52 pp.

Delaney, A.J., 1987. Preparation and description of a research geophysical borehole site containing massive ground ice near Fairbanks, Alaska. Hanover, New Hampshire, U.S. Army CRREL Special Report 87-7, 22 pp.

Delaney, A.J., & Arcone, S.A., 1984. Dielectric measurements of frozen silt using time domain reflectometry. Cold Regions Science and Technology, 9: 37-49.

Dick, R.A., 1970. Effects of type of cut, delay and explosive on underground blasting in frozen gravel. U.S. Bureau of Mines Report of Investigations 7356, 17 pp.

Dostovalov, B.N., and Popov, A.I., 1966. Polygon systems of ice wedges and conditions of their development. Permafrost: International Conference Proceedings, National Academy of Sciences – National Research Council, Washington, DC, Publication 1287: 102-105.

Dubikov, G.I., 2002. Composition and cryogenic structure of permafrost in West Siberia. Moscow: GEOS, 246 pp (in Russian).

Fortier, D., Allard, M., & Shur, Y., 2007. Observation of rapid drainage system development by thermal erosion of ice wedges on Bylot Island, Canadian Arctic Archipelago. Permafrost and Periglacial Processes 18 (3): 229-243.

Fortier, D., Kanevskiy, M., & Shur, Y., 2008. Genesis of Reticulate-Chaotic Cryostructure in Permafrost. Proceedings of the Ninth International Conference on Permafrost (in press).

French, H.M., 2007. The Periglacial Environment, Third Edition. John Wiley and Sons Ltd, Chichester, UK, 458 pp.

Garbeil, H.M., 1983. Temperature effects upon the closure of a gravel room in permafrost. MS thesis, University of Alaska Fairbanks.

Gasanov, S.S., 1963. Morphogenetic classification of cryostructures of frozen sediments. Trudy SVKNII, Vol. 3, Magadan (in Russian).

Gasanov, S.S., 1969. Structure and history of formation of permafrost in Eastern Chukotka. Moscow: Nauka, 168 pp. (in Russian).

Gravis, G.F., 1969. Slope sediments of Yakutia. Moscow: Nauka, 128 pp. (in Russian).

Hamilton, T.D., Ager, T.A., & Robinson, S.W., 1983. Late Holocene ice wedges near Fairbanks, Alaska, USA: environmental setting and history of growth. Arctic and Alpine Research 15 (2): 157-168.

Hamilton, T.D., Craig, J.L., & Sellmann P.V., 1988. The Fox permafrost tunnel: a late Quaternary geologic record in central Alaska. Geological Society of America Bulletin 100: 948-969.

Huang, S.L., Aughenbaugh, N.B., and Wu, M.C., 1986. Stability study of CRREL permafrost tunnel. Journal of Geotechnical Engineering 112: 777-790.

Johansen, N.I., Chalich, P.C., and Wellen, E.W., 1981. Sublimation and its control in the CRREL permafrost tunnel. Hanover, New Hampshire, U.S. Army CRREL Special Report 81-8, 12 pp.

Johansen, N.I., and Ryer, J.W., 1982. Permafrost creep measurements in the CRREL tunnel. Proceedings of the Third International Symposium on Ground Freezing, Hanover, New Hampshire, 1982. Hanover, New Hampshire, U.S. Army CRREL, 61-63.

Kanevskiy, M., 2003. Cryogenic structure of mountain slope deposits, northeast Russia. Proceedings of the Eighth International Conference on Permafrost, Zurich, Switzerland, July 21-25, 2003 1: 513-518.

Kanevskiy, M., Fortier, D., Shur, Y., Bray, M., and Jorgenson, T., 2008. Detailed Cryostratigraphic Studies of Syngenetic Permafrost in the Winze of the CRREL Permafrost Tunnel, Fox, Alaska. Proceedings of the Ninth International Conference on Permafrost (in press).

Katasonov, E.M., 1962. Cryogenic textures, ice and earth wedges as genetic indicators of perennially frozen Quaternary deposits. Issues of Cryology in Studies of Quaternary Deposits. Moscow: Izd-vo AN SSSR, 86–98 (in Russian).

Katasonov, E.M., 1969. Composition and cryogenic structure of permafrost. National Research Council of Canada, Ottawa, Technical Translation 1358, 25-36.

Katasonov, E.M., 1978. Permafrost-facies analysis as the main method of cryolithology. Proceedings of the Second International Conference on Permafrost, July 13-28, 1973. USSR Contribution. Washington: National Academy of Sciences, 171-176.

Katayama, T., Tanaka, M., Moriizumi, J., Nakamura, T., Brouchkov, A., Douglas, T. A., Fukuda, M., Tomita, F., and Asano, K., 2007. Phylogenetic analysis of bacteria preserved in a permafrost ice wedge for 25,000 years. Appl. Environ. Microbiol. 2007 April, 73(7): 2360–2363.

Kudryavtsev, V.A., (ed.). 1978. General Permafrost Science (Geocryology). 2nd edn. Moscow: Moscow University Press, 463 pp. (in Russian).

Lawson, D.E., 1983. Ground ice in perennially frozen sediments, northern Alaska. In: Proceedings of the Fourth International Conference on Permafrost. National Academy Press, Washington, D.C.: 695-700.

Linell, K.A., and Lobacz, E.F., 1978. Some experiences with tunnel entrances in permafrost. Proceedings of the Third International Conference on Permafrost, Edmonton, July 10-13, 1978. Ottawa: National Research Council of Canada, 814-819.

Long, A., and Péwé, T.L., 1996. Radiocarbon dating by high-sensitivity liquid scintillation counting of wood from the Fox permafrost tunnel near Fairbanks, Alaska. Permafrost and Periglacial Processes 7: 281-285.

Mackay, J.R., 1972. The world of underground ice. Annals, Association of American Geographers 62: 1-22.

Mackay, J.R., 1995. Ice wedges on hillslopes and landscape evolution in the late Quaternary, western Arctic coast. Canadian Journal of Earth Sciences, 32: 1093-1105.

Mackay, J.R., 1997. A full-scale experiment (1978-1995) on the growth of permafrost by means of lake drainage, western Arctic coast: a discussion of the method and some results. Canadian Journal of Earth Sciences, 34: 17-33.

Melnikov, V.P., and Spesivtsev, V.I., 2000. Cryogenic Formations in the Earth's Lithosphere. Novosibirsk: Siberian Publishing Center UIGGM, Siberian Branch, Russian Academy of Sciences, 343 pp.

Murton, J.B., and French, H.M., 1994. Cryostructures in permafrost, Tuktoyaktuk coastlands, western arctic Canada. Canadian Journal of Earth Sciences 31: 737–747.

Pettibone, H.C., and Waddell, G.G., 1971. Stability of an underground room in frozen gravel. In Proceedings of the 9th Annual Engineering Geology and Soils Engineering Symposium, Boise, Idaho. Boise, Idaho Department of Highways: 3-30.

Pettibone, H.C., and Waddell, G.G., 1973. Stability of an underground room in frozen gravel. Proceedings, American contribution, Second International Conference on Permafrost: Yakutsk, U.S.S.R. Publication 2115. National Academy of Science, Washington, DC: 699-706.

Péwé, T.L., 1966. Ice wedges in Alaska – classification, distribution and climatic significance. Permafrost: International Conference Proceedings, National Research Council of Canada - National Academy of Sciences, Washington, DC, Publication 1287, 76-81.

Péwé, T.L., 1975. Quaternary geology of Alaska. United States Geological Survey, Professional Paper 835, 145 pp.

Pikuta, E.V., Marsik, D., Dej, A., Tang, J., Krader, P. & Hoover, R. B. 2005. Carnobacterium pleistocenium sp. nov., a novel psychrotolerant, facultative anaerobe isolated from permafrost of the Fox Tunnel in Alaska. Int. J. Syst. Evol. Microbiol., 55, 473-478.

Popov, A.I., 1967. Cryogenic phenomena in the Earth crust (Cryolithology). Moscow: Moscow University Press, 304 pp. (in Russian).

Popov, A.I., 1973. Album of cryogenic formations in the Earth's crust and relief. Moscow: Moscow State University, 56 pp. (in Russian).

Popov, A.I., Rozenbaum, G.E., and Tumel, N.V., 1985. Cryolithology. Moscow: Moscow University Press, 239 pp. (in Russian).

Romanovskii, N.N., 1993. Fundamentals of cryogenesis of lithosphere. Moscow: Moscow University Press, 336 pp. (in Russian).

Sellmann, P.V., 1967. Geology of the USA CRREL permafrost tunnel, Fairbanks, Alaska. Hanover, New Hampshire, US Army CRREL, Technical Report 199, 22 pp.

Sellmann, P.V., 1972. Geology and properties of materials exposed in the USA CRREL permafrost tunnel. Hanover, New Hampshire, US Army CRREL, Special Report 177, 16 pp.

Shumskii, P.A., 1959. Ground (subsurface) ice. In: principles of geocryology, Part I. General geocryology. Academy of Sciences of the USSR, Moscow, Chapter IX, 274-327 (in Russian) (English translation: C. de Leuchtenberg, 1964. National research Council of Canada, Ottawa, Technical Translation 1130, 118 pp).

Shur Y.L., 1988. Upper horizon of the permafrost soils and thermokarst. Novosibirsk: Nauka, Siberian Branch, 210 pp. (in Russian).

Shur, Y., French, H.M., Bray, M.T., and Anderson, D.A., 2004. Syngenetic permafrost growth: cryostratigraphic observations from the CRREL Tunnel near Fairbanks, Alaska. Permafrost and Periglacial Processes 15 (4): 339-347.

Shur, Y., and Jorgenson, M.T., 1998. Cryostructure development on the floodplain of the Colville River Delta, Northern Alaska. Proceedings of the Seventh International Conference on Permafrost, June 23-27, 1998, Yellowknife, Canada. Université Laval, Québec: 993-999.

Soloviev, P.A., 1959. Permafrost of northern part of Lena-Amga plain. Moscow: Academy of Sciences of the USSR Publishing House, 144 pp (in Russian).

Swinzow, G..K. 1970. Permafrost tunnelling by a continuous mechanical method. Hanover, New Hampshire, US Army CRREL, Technical Report 221, 37 pp.

Thompson, E. G. & Sayles, F. H. 1972. In-situ creep analysis of room in frozen soil. Journal of Soil Mechanics and Foundation Division, ASCE, 98: 899-915.

Vasil'chuk, Y.K., and Vasil'chuk, A.C., 1997. Radiocarbon dating and oxygen isotope variations in Late Pleistocene syngenetic ice wedges, Northern Siberia. Permafrost and Periglacial Processes, 8: 335-345.

Vasil'chuk, Y.K., and Vasil'chuk, A.C., 2000. AMS-dating of Late Pleistocene and Holocene syngenetic ice wedges. Nuclear Instruments and Methods in Physics Research B 172: 637-641.

Vtyurin, B.I. 1964. Cryogenic structure of Quaternary deposits. Moscow: Nauka, 151 pp. (in Russian).

Watanabe, O., 1969. On permafrost ice. Journal of Japanese Society of Snow and Ice 31 (3): 53-62 (in Japanese, translated by CRREL).

Weerdenburg, P.C., and Morgenstern, N.R., 1983. Underground cavities in ice-rich frozen ground. Proceedings of the Fourth International Conference on Permafrost, Fairbanks, Alaska, July 17-22, 1983. Washington, D.C.: National Academy Press, 1384-1389.

Wooler, M.J., Zazula, G.D., Edwards, M., Froese, D.G., Boone, R.D., Parker, C., and Bennett, B., 2007. Stable carbon isotope compositions of eastern Beringian grasses and sedges: investigating their potential as paleoenvironmental indicators. Arctic, Antarctic and Alpine Research 39 (2): 318-331.

Zhestkova T.N., 1982. Formation of the cryogenic structure of ground. Moscow: Nauka, 209 pp. (in Russian).

To learn more about the CRREL permafrost tunnel, visit:
http://www.crrel.usace.army.mil/permafrosttunnel/

To learn more about INE research on frozen soils, visit:
http://www.uaf.edu/ine

UAF™ UNIVERSITY OF ALASKA FAIRBANKS